Optimal Sizing of On-Board Energy Storage Devices for Electrified Railway Systems

Chaoxian Wu, Shaofeng Lu*, Fei Xue, Lin Jiang and Minwu Chen

***Abstract*—For improving the energy efficiency of railway systems, on-board energy storage devices (OESDs) have been applied to assist the traction and recover the regenerative energy. This paper aims to address the optimal sizing problem of OESDs to minimize the catenary energy consumption for practical train operations. By employing a mixed integer linear programming (MILP) model based on energy flow and the law of conservation of energy, three types of widely used OESD: supercapacitors, Li-ion batteries and flywheels have been studied in a real-world case of Beijing Changping line. Results show that without the constraints of capital cost and volume, the supercapacitor, Li-ion battery and flywheel with optimized capacity can save the catenary energy consumption by 23.6%, 22.9% and 23.7% compared to the cases without OESDs respectively. The minimum catenary energy consumption for each type of OESD has also been found with the constraints of capital cost and volume. The study shows that with a volume constraint less than 0.6 m^3 and a higher allowed capital cost more than 20 k$, flywheel tends to achieve the least catenary energy consumption. When the volume is relaxed to go beyond 0.6 m^3, supercapacitors always achieve the minimum catenary energy consumption disregarding the constraint of capital cost.**

***Index Terms*—On-board energy storage device (OESD), optimal sizing, electrified railway systems, mixed integer linear programming (MILP), energy-saving**

I. Introduction

For improving the energy efficiency of railway systems, as an emerging application, on-board energy devices (OESDs) have been used in many existing urban rail transit systems nowadays to help recover more regenerative energy as well as power the train by using the stored energy [1]. When compared with other energy-saving measures including energy-efficient driving, stationary energy storage utilization, improving traction efficiency and so on, energy saving rate of OESD is claimed to be the highest, which can reach up to 25% at a system level [2].

There are three types of OESD commonly utilized in modern electrified railway systems around the world: supercapacitors, electrochemical batteries and flywheels. Supercapacitors are widely utilized in urban rail transit systems due to its relatively higher power density, short discharging/charging time, low maintenance cost and long life time [3]. Many urban rail transit systems have been equipped with supercapacitors, such as Brussels tram line, Brussels metro line, Madrid metro line, Blackpool tramway, Mannheim tramway and Paris tram line. The energy saving rate by using supercapacitors ranges from 16% to 35.8% in theoretical assessments [4]–[9]. Electrochemical batteries, such as lead-acid batteries, Ni-Cd batteries, NiMH batteries, Li-ion batteries and so on, are with relatively high energy density leading to large energy-storage capability [1]. Due to this characteristic, electrochemical batteries, referred short to as "batteries", are widely used as stationary energy storage to absorb the regenerative energy from different trains in specific electrified section. It is also used and tested as OESD in some urban rail transit systems, e.g. Sapporo Li-ion battery-driven light rail [10] and Ni-MH battery-driven Catadis tramway in Nice, France [11], and it has brought up to 30% energy saving in industry. Flywheels are featured with a fast charging/discharging time, a virtually infinite number of cycles and offer high energy and power densities [1]. Though flywheel as OESD is still at the early development stage [12], they have been studied in heavy haul trains [13] and also in light rail vehicles [14], achieving an energy saving rate ranging from 9.83% to 31.21%. Based on the above discussion, it can be seen that supercapacitors are the most popular OESD utilized in railway systems, batteries are preferred to be applied as stationary energy storage and embedded flywheels as OESD are still at the early development stage and demands further explorations.

Since the OESDs have been put into use or tested in railway industries, the academic research on the emerging integrated system is becoming increasingly popular. One of the recent research direction in these years is to find the optimal train operation considering embedded OESD. Miyatake *et al.* [15], [16] investigate the optimal train speed with supercapacitor as OESD. In both papers, optimal train speed profiles are found with the modeled circuits of supercapacitor. Huang *et al.* [17] explore the energy-saving potential of supercapacitor by optimizing the train speed profiles from the viewpoint of energy flow. For the battery-driven trains, the optimal solution for train operation with Li-ion battery are also studied by Ghaviha *et al.* [18]. A general integrated optimization model for train with a general model of OESD is proposed by Wu *et al.* [19] with high energy-saving rate and computational efficiency. The work is extended in [20] and the management of OESD at stations and train speed profiles are investigated, which shows that appropriate charging/discharging management in inter-station journeys and dwelling are both important. One common feature of the above studies is that the train operation and control of OESD is optimized together for achieving the minimum energy consumption. However, in these papers the OESD capacity is only given as a parameter without considering its suitability for a given railway system.

Locating the suitable capacity for energy storage systems has been a popular research topic in the field of electrical engineering, and it has been investigated in the microgrid

(MG) [21]–[23] and electric vehicle (EV) applications [24]–[26]. The main focuses of these papers are to determine the appropriate size of the energy storage systems to reduce or minimize the system's operating cost and investment cost of the energy storage devices. On the other hand, sizing problem of the energy storage in electrified railway systems is still a new research direction for both stationary energy storage and OESD [3]. Optimal sizing problem for stationary and substation-based energy storage has been studied with no constraints on weight and volume of the energy storage devices. In [27], energy storage technologies for Auxiliary-Battery-Based Substations are investigated, in which a Techno-economic model for battery sizing, locating and controlling are proposed to minimize the system's operating cost. For recuperation of the regenerative energy, study on the optimal sizing problem of a stationary hybrid energy storage system combining the batteries and supercapacitors is conducted [28], where the train power profiles, battery cycles and depth of discharge (DOD) are considered. To minimize the trade-off between stationary energy storage capacity and charging power, a sizing methodology is proposed and a barrier method combined with a Newtons method is applied to find the optimal solution [29].

Along with the stationary energy storage systems, OESDs on the other hand are also fast developing and widely applied in railway transportation. It has been argued that oversizing of the OESD might unnecessarily increase mass and volume of the system, whereas undersizing might lead to considerable energy waste [1], [19]. By developing a specific simulation tool to simulate the train vehicle movements, power profiles and OESD control, the OESD sizing problem taking into account the railway traffic volumes is studied in [5], which helps shave peak power, reduce voltage drop and line losses. In [30], the numerical simulations and experimental tests are conducted to investigate the problem, where the size of the OESD is reduced to help shave the voltage peak of the overhead contact line as well as to save the energy consumption. In [31], the optimal sizing problem for a light railway vehicle with an OESD combining batteries and supercapacitors are studied by applying genetic algorithms (GA). The target of it is to minimize the cost of the energy from catenary as well as the initial investment and cycling cost of OESD. It is noted that the above optimal sizing studies are conducted by using simulations, hardware experiments and heuristic algorithms, which would result into an issue of sub-optimality and undermine the energy-saving potential of OESD.

From the literature review above, it can be found that further studies are still needed on the optimization method to address the OESD's optimal sizing problem considering both characteristics of OESD and train operations. This paper aims to develop a new mixed integer linear programming (MILP) model to be solved to determine the optimal capacity of different types of OESD which will minimize the catenary energy consumption for practical electrified railway operations. The contributions of the paper are outlined as follows:

- Three types of popular energy storage, supercapacitors, Li-ion batteries and flywheels, are investigated. The characteristics of OESD e.g. power density and energy density, and the industry-concerned factors e.g. capital cost and volume, are all taken into account in the model.
- By modeling the energy flow of the traction system, the charge/discharge process of the OESD, train operation status, complex route conditions and engineering properties of OESD are formulated into a mathematical programming model, in which the global optimal capacity of OESD can be obtained.
- The real-world train operation data from Beijing Changping line is adopted in the research, which shows the effectiveness of the proposed method in real application. Comprehensive compare and contrast studies are performed between different types and different size of OESD based on the results of the model, offering an inside view on their influences on energy-saving effect to the train operation.

The remainder of the paper is organized as follows: Section II elaborates details of the propose method, where the collection of practical train speed data, energy flow modeling, constraints and objective of the model are shown. Section III covers a real-world case study and a detailed comparative study on optimal sizing problem between different OESDs. Section IV draws the conclusion and discusses the future research directions.

II. Mathematical Modeling

In this section, the formulation of optimal sizing problem of OESD according to practical train speed trajectory data based on MILP approach is elaborated.

A. Modeling Scope

As shown in Figure 1, both the energy from the catenary and the energy stored in the OESD are able to jointly supply the energy needed by the train motor for traction. On the other hand, when the train is conducting regenerative braking, the regenerative energy can be recovered by OESD from the motor. In the proposed model, the energy is not permitted to be fed back to the grid for the sake of simplicity and practicality in view of the power control devices. Due to the limited capacity of the OESD, a proportion of the regenerative energy will be dissipated by the braking resistor. Note that the micro circuit modeling of OESD is not within the scope of this paper.

B. Distance-based Discretization

The inter-station sections in railway line are separated by different stations along with the whole track. The track length D_i for i^{th} inter-station section is first discretized and divided into several distance segments with the value $\Delta d_{i,j}$ respectively, the sum of which satisfies (1).

$$\sum_{j=1}^{N_i} \Delta d_{i,j} = D_i \tag{1}$$

where N_i is the total amount of the divided distance segments for i^{th} inter-station section.

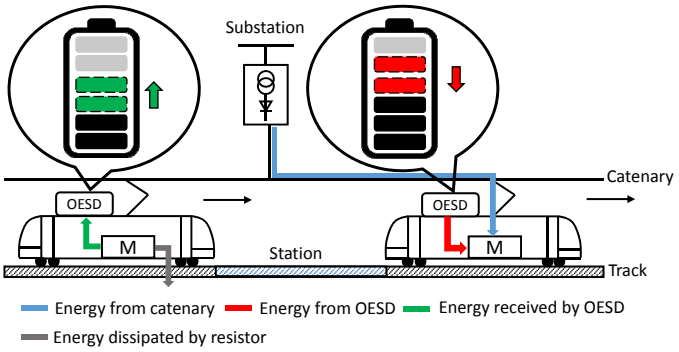

Fig. 1. A schematic diagram of energy flow for operating trains equipped with OESDs

$\Delta d_{i,k}$ can be modified with different value according to practical track conditions e.g. different track length and gradients so that the track length can be fitted. Within one distance segment, there is no change of the gradient. For example, as shown in Figure 2, the whole track length for the i^{th} inter-station journey is 1960 m and the gradient changes occur at 47 m, 380 m, 1510 m and 1805 m. D_i is first divided into 20 distance segments with 19 100-meter segments and 1 60-meter segment without considering the gradient information, shown as the black dash lines in Figure 2. This means that $\Delta d_{i,j}$ for $j = 1...19$ is 100 meters and $\Delta d_{i,20}$ is 60 meters in length. Followed by this, we insert the division lines in gradient switching points mentioned above to do the reconfiguration of $\Delta d_{i,j}$, shown as the red dash lines in Figure 2. After the reconfiguration, the number of $\Delta d_{i,k}$ increases from 20 to 24 with $\Delta d_{i,1}$, $\Delta d_{i,2}$, $\Delta d_{i,3} \sim \Delta d_{i,4}$, $\Delta d_{i,5}$, $\Delta d_{i,6}$, $\Delta d_{i,7} \sim \Delta d_{i,17}$, $\Delta d_{i,18}$, $\Delta d_{i,19}$, $\Delta d_{i,20} \sim \Delta d_{i,21}$, $\Delta d_{i,22}$, $\Delta d_{i,23}$ and $\Delta d_{i,24}$ assigned with 47 m, 53 m, 100 m, 80 m, 20 m, 100 m, 10 m, 90 m, 100 m, 5 m, 95 m, 60 m respectively. Both D_i and $\Delta d_{i,j}$ have no minimum or maximum limits as they are determined by the studied railway systems and field data of the speed profiles. Also, the shorter the $\Delta d_{i,j}$ is, the more speed data to be collected, and the more precise result it will be.

After the discretization of the route, the practical train speed of both ends of each $\Delta d_{i,j}$ can be collected, shown as the circles in Figure 2. As there are N_i distance segment $\Delta d_{i,j}$, there will be $N_i + 1$ collected train speed points $V_{i,1}$, $V_{i,2}$... $V_{i,j}$... V_{i,N_1+1}. Therefore, the average speed $V_{i,j,ave}$ of each $\Delta d_{i,j}$ can be calculated by using the collected $V_{i,j}$ as shown in (2).

$$V_{i,j,ave} = \frac{V_{i,j} + V_{i,j+1}}{2} \tag{2}$$

After having the average speed for each $\Delta d_{i,j}$, the elapsed time $\Delta t_i, j$ for each $\Delta d_{i,j}$ for the inter-station journey can be calculated by using (3).

$$\Delta t_{i,j} = \frac{\Delta d_{i,j}}{V_{i,j,ave}} \tag{3}$$

The drag force $F_{i,j,drag}$ for each $\Delta d_{i,j}$ can be calculated by Davis equation as shown in (4), where A, B and C are the

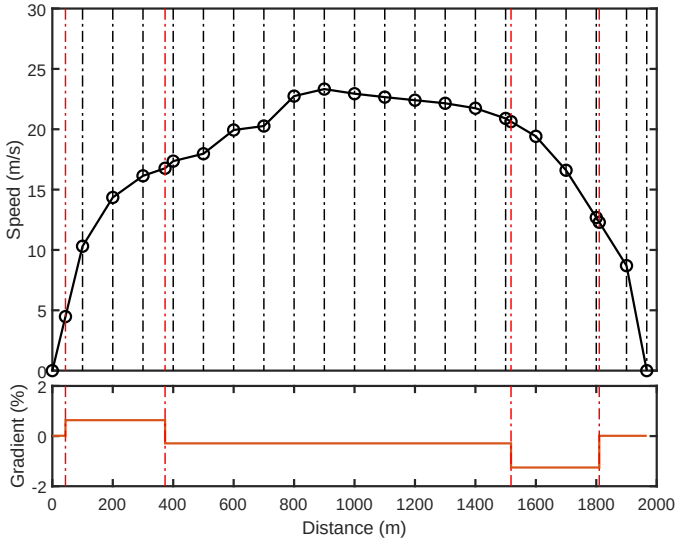

Fig. 2. Schematic illustration of discretization process of the one typical inter-station section. Black solid line is the practical train speed trajectory, black dash lines are the basic division without considering the gradients information, red dash lines are the division imposed by specific gradient change and circles are the corresponding speed points.

Davis coefficients.

$$F_{i,j,drag} = A + BV_{i,j,ave} + CV^2_{i,j,ave} \tag{4}$$

As we can see, through collecting the practical train running speed based on route discretization, the related parameters of this speed trajectory including running time and drag force can be obtained as well by simple calculation, which are the important inputs of the later modeling and optimization process.

C. Energy Flow Modeling of the Train and OESD

The energy flow is transferred between energy sources (catenary and OESD) and train motor. In each $\Delta d_{i,j}$, the train will consume the energy from catenary and OESD or regenerate the energy during braking then feed it back to OESD. Supposing $E_{i,j,m}$ is the traction energy in $\Delta d_{i,j}$. When the train conducts motoring, in each $\Delta d_{i,j}$ the motor consumes the energy from catenary $E_{i,j,c}$ with an efficiency η_1 and the energy discharged by the OESD $E_{i,j,dch}$ with an efficiency η_2, thus $E_{i,j,m}$ can be expressed by the equation shown in (19).

$$E_{i,j,m} = E_{i,j,c} \cdot \eta_1 + E_{i,j,dch} \cdot \eta_2 \tag{5}$$

When the train conducts regenerative braking, in each $\Delta d_{i,j}$ the regenerative energy $E_{i,j,ch}$ would be recovered by OESD with an efficiency η_2. $E_{i,j,r}$ is the energy generated by the motor and transmitted to OESD, which can be expressed by using (6).

$$E_{i,j,r} = \frac{-E_{i,j,ch}}{\eta_2} \tag{6}$$

In this study, it should be noted that η_1 is to specify the total efficiency for motors with the driving system and energy transmission of the power network; similarly, η_2 is to

specify the total efficiency for motors with the driving system and energy conversion from the OESD. An average constant efficiency is adopted in this paper to present a long-term effect.

The state of energy (SOE) defines the amount of stored energy relative to the capacity E_{cap} of the OESD, it is accumulated with the train's running from the first station. It can be expressed based on the proposed model in the study in the equation (7).

$$SOE_{i,j} = \frac{E_{ini} - \sum_{j=1}^{J} E_{i,j,dch} + \sum_{j=1}^{J} E_{i,j,ch}}{E_{cap}} \times 100\% \tag{7}$$

where E_{ini} is the initial available energy in the OESD when the train departs from the first station. In addition, $J = j$, when $i = 1$ for the running at the first inter-station journey; $J = N_1 + N_2 + ... + N_{i-1} + j$, when $i \geq 2$ since the status of the OESD in previous inter-station journeys needs to be accumulated together.

It can be found in [1], [32] and [33] that the performance of the energy storage is commonly expressed by using energy density, power density, capital cost in the unit of "energy per unit mass", energy per unit volume" and "power per unit mass". In this case, the linear relationships among the capacity, mass, maximum discharge/charge power, volume of each type of OESD can be established. As result, Different capacity of the OESD E_{cap} leads to different mass of the OESD M_o, the relationship between the capacity and the mass can be represented in (8).

$$M_o = \frac{E_{cap}}{X_m} \tag{8}$$

where X_m is the energy density with respect to the mass and it is a constant determined by the feature of different types of OESD.

Additionally, the maximum discharging and charging power $\overline{P_o}$ of OESD is related to the mass of it, thus we have the relationship as shown in (9).

$$\overline{P_o} = Y \times M_o = Y\frac{E_{cap}}{X_m} \tag{9}$$

where Y is the power density with respect to the mass and it is a constant determined by the feature of different types of OESD.

Since in the Section II-B the $V_{i,j}$ are collected, the kinetic energy change $E_{i,j,k}$ of the train in each $\Delta d_{i,j}$ can be calculated by using (10).

$$\begin{aligned} E_{i,j,k} &= \frac{1}{2}(M_t + M_o)(V_{i,j+1}^2 - V_{i,j}^2) \\ &= \frac{1}{2}(M_t + \frac{E_{cap}}{X_m})(V_{i,j+1}^2 - V_{i,j}^2) \end{aligned} \tag{10}$$

where M_t is the mass of the train.

The work done by the drag force $E_{i,j,f}$ in each $\Delta d_{i,j}$ can also be obtained as shown in (11).

$$E_{i,j,f} = F_{i,j,drag}\Delta d_{i,j} \tag{11}$$

The potential energy change of the train $E_{i,j,p}$ resulted from the gradient change of the route is calculated by using (12).

$$\begin{aligned} E_{i,j,p} &= (M_t + M_o)g\Delta d_{i,j}\theta_{i,j} \\ &= (M_t + \frac{E_{cap}}{X_m})g\Delta d_{i,j}\theta_{i,j} \end{aligned} \tag{12}$$

where g is the gravitational constant and $\theta_{i,j}$ is the gradient for the interval of $\Delta d_{i,j}$.

D. Constraints and Objective of the Proposed MILP Problem

Mixed integer linear programming (MILP) problem are problems with an objective function and constraints that all linear in the decision variables [34]. Different from the linear optimization problems, at least some of the variables in MILP problems are constrained to take on integer values. The general form of a MILP problem is shown in (13).

$$\begin{aligned} \min \quad & c_0 + \sum_{i=1}^{n} c_i x_i \\ \text{s.t.} \quad & \sum_{i=1}^{n} A_j^e x_i = b_j^e, && \forall j = 1, ..., l_e \\ & \sum_{i=1}^{n} A_j^{ine} x_i \leq b_j^{ine}, && \forall j = 1, ..., l_{ine} \\ & x_i \in \mathbb{Z}, && \text{for some} \quad x_i = 1, ..., n \\ & x_i \in \mathbb{R}, && \text{for the remaining} \quad x_i = 1, ..., n, \end{aligned} \tag{13}$$

where $x_1, ..., x_n$ are the decision variables to be optimized. l_e and l_{ine} are the numbers of equality and inequality constraints. Thus, l_e+l_{ine} is the total number of constraints. The coefficients, A_j^e, A_j^{ine}, l_e and l_{ine}, the terms on the right-hand sides of the constraints, b_j^e and b_j^{ine} and the coefficients, $c_o, ..., c_n$, in the objective function are all constants. Since the optimal sizing of OESD for electrified railway systems is formulated into a MILP problem, the constraints and objective of the model need to be adjusted accordingly with consideration of this specific problem.

According to the law of conservation of the energy, the conversion of the energy can be expressed in (14).

$$E_{i,j,m} + E_{i,j,r} - E_{i,j,k} - E_{i,j,f} - E_{i,j,p} \geq 0 \tag{14}$$

When the train is in traction mode, $E_{i,j,m} \geq 0$, the electrical energy from both the catenary and the OESD are consumed by the motor and converted into the kinetic energy, heat and the potential energy; when the train conducts regenerative braking, $E_{i,j,r} \leq 0$, the kinetic energy is converted into heat, the potential energy and electrical energy which is recovered by the OESD.

Since motoring and braking cannot occur at the same time, to distinguish different train operation modes, the integer variables $\lambda_{i,j}$ are introduced and (15), (16), (17) and (18) need to be imposed.

$$E_{i,j,c} \cdot \eta_1 \leq \lambda_{i,j} L_1 \tag{15}$$

$$E_{i,j,dch} \cdot \eta_2 \leq \lambda_{i,j} L_1 \tag{16}$$

$$\frac{E_{i,j,ch}}{\eta_2} \leq (1-\lambda_{i,j})L_2 \tag{17}$$

$$\lambda_{i,j} = 0 \quad or \quad 1 \tag{18}$$

These constraints ensure that when there are $E_{i,j,c}$ and $E_{i,j,dch}$, there is no $E_{i,j,ch}$ existing at the same time, and vice versa. L_1 and L_2 are two sufficiently large numbers to ensure a valid range of these variables.

In addition to the energy restriction, the power limit of the motor and OESD should be added as the constraints respectively. For the motor, (19) and (20) is used to ensure the power that the motor supplies in both traction mode and braking mode does not exceed the maximum traction power $\overline{P_t}$ and maximum regenerative braking power $\overline{P_b}$.

$$E_{i,j,c} \cdot \eta_1 + E_{i,j,dch} \cdot \eta_2 \leq \overline{P_t}\Delta t_{i,j} \tag{19}$$

$$\frac{E_{i,j,ch}}{\eta_2} \leq \overline{P_b}\Delta t_{i,j} \tag{20}$$

For the OESD, the power for the discharged and charged energy cannot exceed the maximum charge and discharge power.

$$E_{i,j,dch} \leq \overline{P_o}\Delta t_{i,j} = Y\frac{E_{cap}}{X_m}\Delta t_{i,j} \tag{21}$$

$$E_{i,j,ch} \leq \overline{P_o}\Delta t_{i,j} = Y\frac{E_{cap}}{X_m}\Delta t_{i,j} \tag{22}$$

Additionally, the work done by the motor need to be restricted by the maximum traction force provided by the motor $\overline{F_t}$ and the maximum braking force $\overline{F_b}$ as well. (23) and (24):

$$E_{i,j,c} \cdot \eta_1 + E_{i,j,dch} \cdot \eta_2 \leq \overline{F_t}\Delta d_{i,j} \tag{23}$$

$$\frac{E_{i,j,ch}}{\eta_2} \leq \overline{F_b}\Delta d_{i,j} \tag{24}$$

The stored energy in the OESD cannot lower than 0 and higher then 100%, thus constraint (25) needs to be added into the model.

$$0 \leq SOE_{i,j} \leq 100\% \tag{25}$$

In addition, the initial SOE of the OESD when the train departs from the first station should be 0 thus we have constraint (26).

$$E_{ini} = 0 \tag{26}$$

It can be seen above that the continuous variables are E_{cap}, E_{ini}, $E_{i,j,c}$, $E_{i,j,dch}$ and $E_{i,j,ch}$, the integer variables are $\lambda_{i,j}$, the equality constraints of the model are (18) and (26), and the inequality constraints are (14)-(17) and (19)-(25). The objective function of the entire model is the net energy consumption which is the difference of the total traction energy consumption (The sum of total catenary energy consumption and total discharged energy from OESD) and the total regenerative energy received by OESD, as shown in (27). By conducting this optimization to minimize the net energy consumption, catenary energy consumption is also minimized.

$$\begin{aligned} \min \quad & \sum_{i=1}^{I}\sum_{j=1}^{N_i}(E_{i,j,c} + E_{i,j,dch} - E_{i,j,ch}), \\ \text{s.t.} \quad & (14)-(26). \end{aligned} \tag{27}$$

Fig. 3. The route map for Beijing Changping line

TABLE I
THE INTER-STATION LENGTH AND THE DISTANCE INTERVAL USED IN SPEED DATA COLLECTION FOR BEIJING CHANGPING LINE

Inter-station name	Length (m)	Distance interval (m)
XRQ-LP	5441	200
LP-ZXZ	2368	100
ZXZ-GHC	3810	200
GHC-SH	2037	100
SH-SUP	1967	100
SUP-NS	5364	200

TABLE II
THE ENERGY DENSITY PER UNIT MASS/VOLUME, POWER DENSITY PER UNIT MASS AND CAPITAL COST PER UNIT ENERGY CAPACITY FOR THREE TYPES OF OESD [1]

OESD type	Energy density		Power density	Capital cost
	(kWh/t)	(kWh/m^3)	(kW/t)	($/kWh)
Supercapacitor	2.5-15	10-30	500-5000	300-2000
Li-ion battery	75-200	150-500	100-350	500-2500
Flywheel	5-100	20-80	1000-5000	1000-5000

where I is the total number of the investigated inter-station sections.

The proposed MILP model can be solved by commercial solver e.g. CPLEX® and Lingo®, etc. efficiently to determine the optimal capacity of the OESD and to minimize the catenary energy consumption.

III. CASE STUDIES AND RESULTS DISCUSSION

In this section, the effectiveness of the proposed approach is demonstrated by using a real case study based on the data from Beijing Changping line. The Changping line covers 21 kilometers distance and has 7 stations. The route map for the Changping line is shown in Figure 3 and Figure 4 illustrates the traction/braking characteristics, basic drag force of the train and gradient information of the route [35]. The practical train speed trajectory for each inter-station section of the Changping line and corresponding distance interval for speed data collection follow the literature [36]. These information has been integrated and tabulated in Table I.

The case studies mainly focus on the three types of OESD, namely supercapacitor, battery and flywheel due to their most

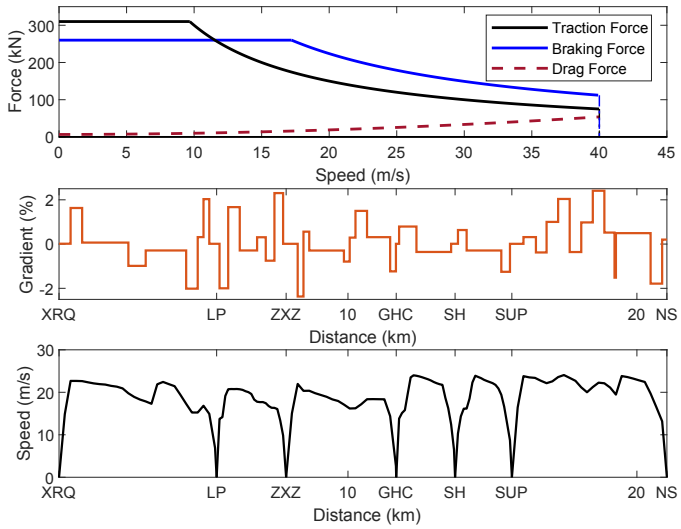

Fig. 4. The traction/braking characteristics of the train motor, drag force, gradient information and practical train speed trajectory of the Changping line

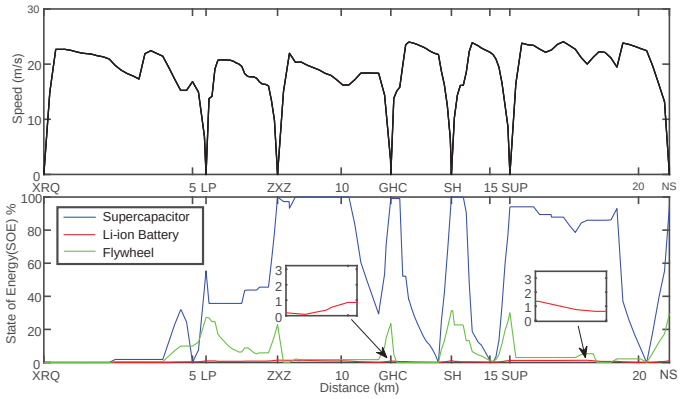

Fig. 5. The reference train speed trajectories and discharge/charge curves for different optimally sized OESD without constraints of capital cost and volume

TABLE III
OPTIMIZATION RESULTS OF CENTENARY ENERGY CONSUMPTION AND OESD CAPACITY FOR CASE WITHOUT CONSTRAINTS OF CAPITAL COST AND VOLUME

OESD type	Optimal capacity (kWh)	Minimum catenary energy consumption (kWh)	Energy-saving rate* (%)
Supercapacitor	10.1	157.3	23.6
Li-ion battery	923.8	158.9	22.9
Flywheel	32.0	157.2	23.7

*The energy-saving rate of catenary energy consumption with optimally sized OESD in reference to the scenario without OESD.

TABLE IV
THE VOLUME, CAPITAL COST, MAXIMUM POWER AND MASS OF THE OPTIMALLY SIZED OESDS FOR CASE WITHOUT CONSTRAINTS OF CAPITAL COST AND VOLUME

	OESD type		
	Supercapacitor	Li-ion battery	Flywheel
Volume (m^3)	0.5	2.8	0.6
Capital cost (k$)	11.6	1385.8	96.1
Maximum power (kW)	877.5	419.9	508.2
Mass (t)	0.32	1.87	0.17

popular applications. In addition, Li-ion battery is selected to represent the other types of chemical battery. The main parameters for three types of OESD are from [1] and listed in Table II. The data used in the case studies have been checked by referring to literature [1], [32] and [33] of the energy storage technologies development and their applications. In these three review articles, the values of each parameter share large intersections. Additionally, [1] is the latest review article of the energy storage technologies already utilized in specifically railway systems, thus, the data from it are used in case studies. It should be noted that for the purpose of a general investigation, the halfway point of these ranges is selected e.g. the power density for supercapacitor used in the case studies is set to be $(500 + 5000)/2 = 2750$ kW/t. This halfway point value is considered as one of the reasonable presentations of the general characteristics of one type of energy storage. This value needs to be updated to reflect the technical development of energy storage technology and maintain a high level of modeling accuracy. With the fast development of energy storage technologies, the general performance of these three types of OESD will see substantial progresses and this halfway point will definitely change in the foreseeable future. The proposed model still can be used to obtain the corresponding new optimal size of the OESD based on the new values of these parameters.

The mass of the train in the Changping line is 194.3 ton and the average energy efficiency η_1 and η_2 can be set based on literature from long-term viewpoint. Specifically, the energy transmission efficiency from grid to the motor is set as 90% due to a 10% average energy loss and the energy conversion efficiency of electric motor is set as 90% for most typical engineering applications [2]. Therefore, the approximated value for η_1 is 81% = 90% $\times$ 90% in this study. On the other hand, energy can be directly transmitted between the motor and OESD with a negligible transmission loss [1], thus, the value for η_2 is set as 90% considering only the discharge/charge efficiency resulted from the OESD's own resistance. Both values can be modified according to the field data collected from different types of power supply system, different rolling stocks and different types of OESD.

Note that the case studies are conducted by using Matlab R2018b® and CPLEX® 12.8.0 solver on a PC with Intel Core® i5-6500 processor (3.20 GHz) and 8.00 GB RAM.

A. Without the constraints of capital cost and volume

Regardless of the capital cost and volume of the OESD, the reference train speed trajectories for the Changping line and its optimal discharge/charge curves represented by OESDs' SOE are shown in Figure 5. The optimal capacity of each type of OESD and respective catenary energy consumption are tabulated in Table III, and the corresponding resulted volume, capital cost, maximum power and mass are also given in Table IV.

From the Table III it is observed that without any constraints on capital cost and volume, with the same reference speed

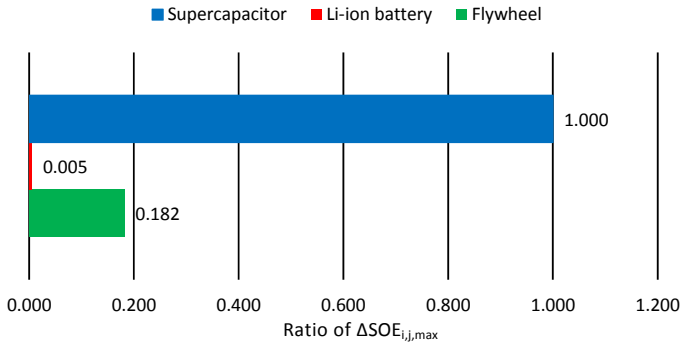

Fig. 6. The ratio among $\Delta SOE_{i,j,max}$ of each type of OESD regarding supercapacitor as base value for the case without the constraints of capital cost and volume

TABLE V
THE ENERGY-SAVING RATE WITH RESPECT TO THE CAPACITY, VOLUME AND CAPITAL COST OF OPTIMALLY SIZED OESDS FOR CASE WITHOUT CONSTRAINTS OF CAPITAL COST AND VOLUME

	OESD type		
	Supercapacitor	Li-ion battery	Flywheel
Energy-saving rate per unit capacity (%/kWh)	2.35	0.02	0.74
Energy-saving rate per unit capital cost (%/k$)	2.05	0.02	0.25
Energy-saving rate per unit volume (%/m^3)	47.07	8.04	37.01

trajectories, supercapacitor, Li-ion battery and flywheel with respective optimal capacity can bring the similar energy-saving effect, reducing catenary energy consumption by 23.6%, 22.9% and 23.7% respectively. However, the optimal OESD capacity sees substantial differences when compared among different types of OESD. For achieving the minimum catenary energy consumption, the optimal capacity for Li-ion battery is extremely high, which reaches 923.8 kWh, and for supercapacitor is the lowest being 10.1 kWh. In addition, results shown in Table IV also bring some valuable information about each OESD under this optimal capacity. For example, among the three the Li-ion battery is the heaviest and the most space-consuming, which needs much space for installation even though its division into several sets, and flywheel is the lightest and supercapacitor is the most space-efficient in this case. Though the optimal capacity of Li-ion battery is the highest, maximum power of it is still the lowest among the three, showing the low power support which is the commonly recognized drawback of the chemical battery. The capital cost for Li-ion battery becomes the most significant factor with an extremely high value of 1385.8 k$, which is also impractical in the real operation. In short, adoption of Li-ion battery demands higher economic cost and larger space to achieve the optimal capacity.

From Figure 5, it can also be seen that the discharge/charge curves for these three types of OESDs are also different. The maximum gradient of SOE curves for supercapacitor is much higher than the other two types of OESDs, depicting a much steeper curves than the other. The SOE curve for Li-ion battery

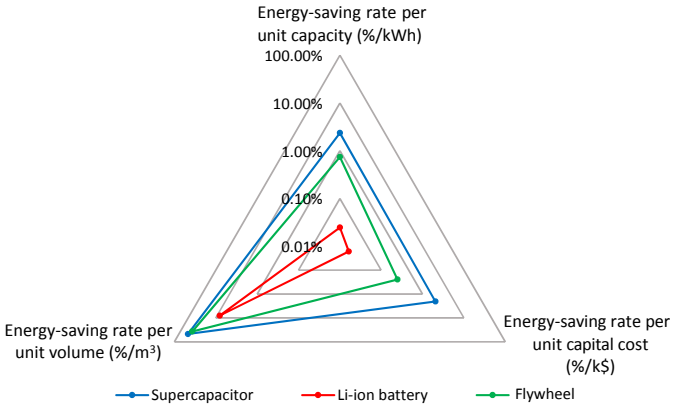

Fig. 7. The radar chart for comparison among the energy saving rate with respect to the optimal capacity, volume and capital cost for the case without constraints of capital cost and volume.

is enlarged for a clear view in the figure since the change of it is hard to be observed. The maximum increment or decrement of SOE in each $\Delta d_{i,j}$, notated as $\Delta SOE_{i,j,max}$, is determined by the equation (28).

$$\Delta SOE_{i,j,max} = \overline{P_o}\Delta t_{i,j}/E_{cap} \tag{28}$$

From Table IV it is seen that supercapacitor is with the highest discharge/charge power, flywheel ranks the second and Li-ion battery is with the lowest maximum power while the trend for their respective capacity is exactly contrary. As a result, this leads to the different $\Delta SOE_{i,j,max}$ when different type of OESD is investigated. If the $\Delta SOE_{i,j,max}$ for supercapacitor is regarded as the base value, the ratio of $\Delta SOE_{i,j,max}$ for supercapacitor, Li-ion battery and flywheel can be obtained as 1: 0.005: 0.182, as shown in Figure 6, clarifying the reason for the significantly different discharge/charge curve for each type of OESD. It also should be noted that due to the low power density of the Li-ion battery, the obtained optimal solution results in a relatively high maximum power for it while with a extremely large capacity. In this case, though using Li-ion battery can bring the similar energy-saving effect as the supercapacitor and flywheel do, there is still more than 90% of the capacity of it not being used.

Since the optimal capacity, volume and capital cost of three types of OESD are obtained, the energy-saving efficiency from the industry viewpoint related to these three important factors can be studied. Here three terms, energy-saving rate per unit capacity in %/kWh, energy-saving rate per unit capital cost in %/k$ and energy-saving rate per unit volume in %/m^3, are proposed and obtained, as shown in Table V. Additionally, the comparison among each value of them are made into a radar chart illustrated in Figure 7. From the figure, it can be observed that supercapacitor is the most efficient in reduction of caternary energy consumption in terms of the above three aspects while Li-ion battery seems to be with low efficiency to save energy consumption. In terms of energy-saving rate per unit volume, performance of flywheel is close to that of supercapacitor.

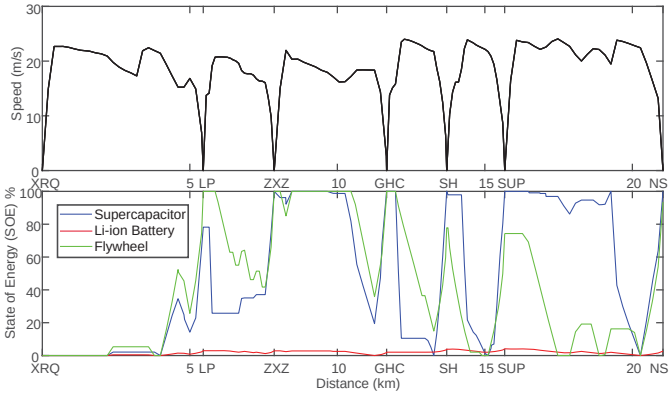

Fig. 8. The reference train speed trajectories and discharge/charge curves for different optimally sized OESD with upper limit of capital cost being 10 k$

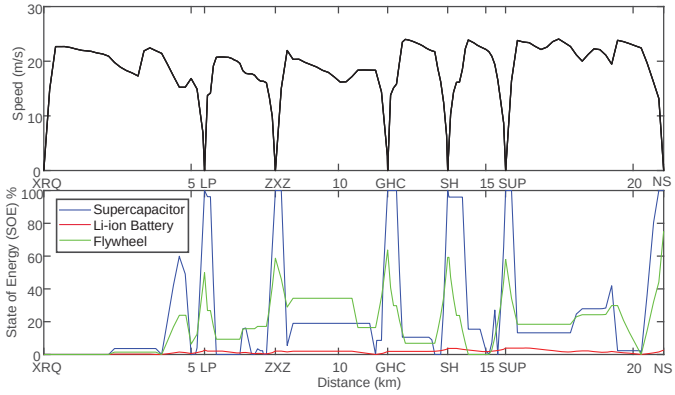

Fig. 9. The reference train speed trajectories and discharge/charge curves for different optimally sized OESD with upper limit of volume being 0.25 m^3

TABLE VI
OPTIMIZATION RESULTS OF CAPACITY, ENERGY SAVING RATE, VOLUME, CAPITAL COST, MAXIMUM POWER AND MASS FOR DIFFERENT OESDS WITH AN UPPER LIMIT OF CAPITAL COST OF 10 K$

	OESD type		
	Supercapacitor	Li-ion battery	Flywheel
Optimal capacity (kWh)	8.7	6.7	3.3
Energy-saving rate (%)	22.5	0.5	8.3
Volume (m^3)	0.44	0.02	0.07
Capital cost (k$)	10	10	9.9
Maximum power (kW)	758.7	3.0	52.9
Mass (t)	0.28	0.01	0.02

TABLE VII
OPTIMIZATION RESULTS OF CAPACITY, ENERGY SAVING RATE, VOLUME, CAPITAL COST, MAXIMUM POWER AND MASS FOR DIFFERENT OESDS WITH AN UPPER LIMIT OF VOLUME OF 0.25 m^3

	OESD type		
	Supercapacitor	Li-ion battery	Flywheel
Optimal capacity (kWh)	5.0	81.3	12.5
Energy-saving rate (%)	16.9	5.8	19.9
Volume (m^3)	0.25	0.25	0.25
Capital cost (k$)	5.8	121.9	37.5
Maximum power (kW)	436.5	36.9	198.4
Mass (t)	0.16	0.16	0.07

B. With the constraints of capital cost and volume

In Section III-A, it can be found that without the constraint of capital cost ad volume, Li-ion battery, supercapacitor and flywheel can bring a very similar energy-saving effect through the optimized capacity. However, this also leads to an impractical capital cost for Li-ion battery and even for flywheel who reaches 96.1 k$. In addition, the resulted volume for Li-ion battery is also with large value. In real business, railway operators need to take into account the company budget and left space on the rail vehicles when applying OESD, and normally different companies have different requirements. As a result, in this section the upper limits of the cost being 10 k$ and volume being 0.25 m^3 are selected firstly for showing the practicality and flexibility of the proposed method. This case study with the constraints of capital cost and volume shows that the proposed method can meet different needs of varies of operators with different investment and installation requirements.

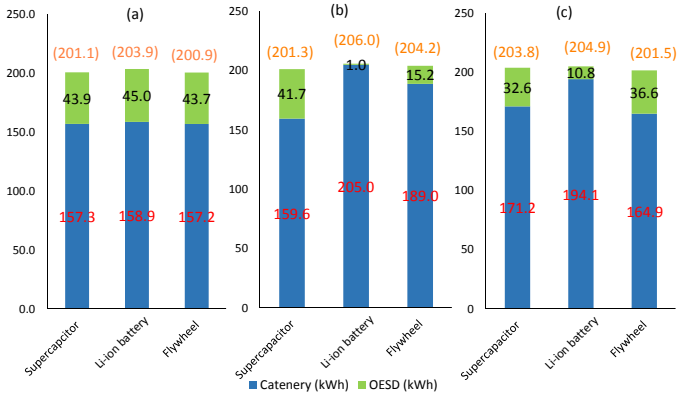

Fig. 10. Traction energy supply split between catenary and OESD in the optimization results under different constraints. (a) No constraints of capital cost and volume imposed; (b) With a capital cost upper limit of 10 k$; (c) With a volume upper limit of 0.25 m^3 (The orange value in parentheses is the total traction energy consumption which is the sum of catenary energy consumption and discharged energy from OESD

The optimal results for both scenarios are tabulated in Table VI and Table VII, and the discharge/charge curves are demonstrated in Figure 8 and Figure 9. It can be observed that when the upper limit of capital cost is set to be 10 k$, the most energy-saving OESD is supercapacitor as it has the highest optimal capacity and maximum discharging/charging power in this case. Li-ion battery sees the highest catenary energy consumption as well as with the low maximum power which is only 3.0 kW. Flywheel is with least optimal capacity since it is more expensive than other. When the upper limit of volume is 0.25 m^3, the most energy-saving OESD becomes flywheel which has the largest optimal capacity. Though Li-ion battery is still with the worst energy-saving effect, the optimal capacity is highest among the three, which indicates a high energy density of its kind. Supercapacitor is with the least optimal capacity, implying its low energy density with respect to the volume constraint. Similar to the case without the constraint of capital cost and volume, the change rate of discharge/charge curves for Li-ion battery in both scenarios here are not significant due to the relatively low maximum power and capacity.

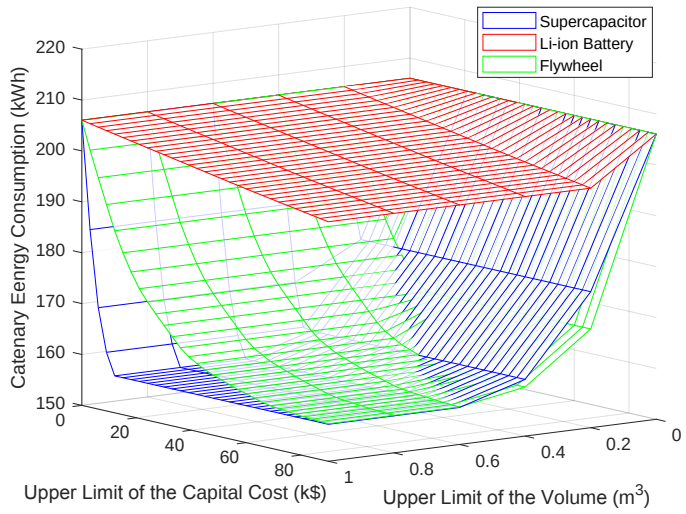

Fig. 11. The catenary energy consumption for different types of OESD under varying upper limits of capital cost and volume

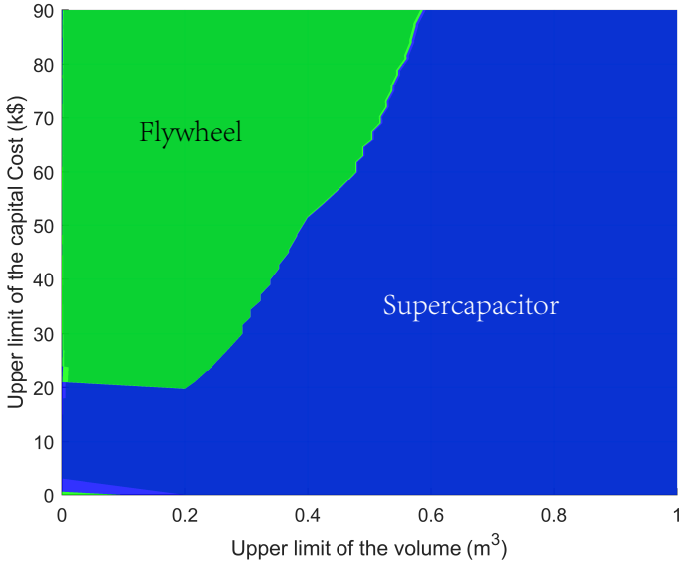

Fig. 12. The different dominated area of minimum catenary energy consumption with respect to upper limits of volume and capital cost (The dominated area of both supercapacitor and flywheel is demonstrated on a projected plane of Figure 11 from the top with x-axis being the volume and y-axis being the capacity cost. By dominating area, it means that adoption of the specific type of OESD will consume the minimum catenary energy consumption among the three).

The energy supply split for each type of OESD is shown in Figure 10, in which the scenarios investigated above are all compared and contrasted. From the figure, it is shown that in different scenario, the energy supply split varies. For the scenario without the constraints of capital cost and volume (Figure 10-(a)), it can be found that though the train equipped with Li-ion battery uses the most catenary energy consumption, Li-ion battery supplies the most energy. From Figure 10-(b) for scenario with an upper limit of capital cost being 10 k$, it is clear that supercapacitor supplies the most energy to train while Li-ion battery hardly support the train due to the low discharging/charging power. The performance of flywheel is also influenced passively by its low capacity. When given the upper limit of volume at 0.25 m^3, flywheel brings the most energy-saving effect and supply the most energy for traction, as shown in Figure 10-(c). The orange values in parentheses are their corresponding total traction energy consumption and it can be seen that in terms of one specific type of OESD, the more energy supplied by OESD, the less total traction energy consumed. This is due to the higher efficiency of using the energy supplied by OESD than using the energy from catenary, which also cuts the catenary energy consumption in turn.

Based on the proposed model, Figure 11 depicts further on the relationship between the catenary energy consumption and capital cost and space of OESD, which are industry-concerned factors. In Figure 11, the range of the upper limit for capital cost is from 0 to 90 k$ with an increment step of 3 k$ and the range of the upper limit for volume is from 0 m^3 to 1 m^3 with an increment step of 0.2 m^3. From the figure, it should be noted that Li-ion battery always gives the highest catenary energy consumption among the three. As for the supercapacitor, the catenary energy consumption for it is the most sensitive with respect to the upper limit of capital cost among the three since it can be noted from the figure that the catenary energy consumption of it drops faster than others when upper limit of capital cost rises. The catenary energy consumption for flywheel is more sensitive and in some space it brings the least catenary energy consumption. The dominated area for minimum catenary energy consumption of supercapacitor and flywheel with respect to capital cost and volume is illustrated in Figure 12 which is a projected plane of Figure 11 from the top. It can be told that with capital cost limited below 20 k$ and volume limitation relaxed to be higher than 0.6 m^3, supercapacitor with optimized capacity brings the minimum catenary energy consumption. When the upper limit of volume is set below 0.6 m^3 and maximum capital cost is allowed to go higher, flywheel with the optimized capacity saves the most catenary energy consumption among the three types of OESD. This result clearly shows that when the installation room is limited, flywheel will be the better choice and if the limitation of the capital cost is tight, supercapacitor is more economic and able to achieve less catenary energy consumption. The result provides a clear guide on how appropriate OESD can be selected for real engineering applications.

IV. Conclusion and Future Work

With the rapid development of energy storage technologies, more and more energy storage has been utilized in railway systems to save energy cost. As a result, on-board energy storage device (OESD), due to its low energy loss, has been used by industry. However, the optimal size of the OESD is still yet to be investigated in the previous research. This paper proposes a mixed integer linear programming (MILP) model to optimize the capacity of the OESD to minimize the catenary energy consumption. Three types of OESD, supercapacitor, Li-ion battery and flywheel, are investigated with different

engineering characteristics including energy density, power density and capital cost.

From the results of the real-world case study, it is found that supercapacitor, Li-ion battery and flywheel can bring similar energy-saving effect, with a reduction rate of catenary energy consumption by 23.6%, 22.9% and 23.7% respectively, without the constraint of capital cost and volume. In cases with constraints on the capital cost and volume, it is found that the energy saving rate for Li-ion battery is significantly reduced compared with supercapacitor and flywheel. When the volume is limited below 0.6 m^3 and capital cost is allowed to be higher than 20 k$, optimally sized flywheel can bring the minimum catenary energy consumption. If the capital cost is constrained below 20 k$ while the volume can be relaxed beyond 0.6 m^3, supercapacitor with optimal capacity brings the most reduction of catenary energy consumption. All in all, based on the proposed method, the optimal capacity of the OESD can be obtained to achieve the minimum catenary energy consumption, the industry-concerned factors that influence the reduction of energy consumption can also be studied, which reveals the impact of different types and different size of OESD on energy-saving effect in electrified railway systems.

In this paper, it is observed that different characteristics of various types of OESD leads to varying energy saving rates and optimal capacities. However, more specific properties e.g. discharge/charge cycle or self-discharge rate of different types of energy storage, which are two important parameters for their strong influence on the overall system costs [1], are not considered in this paper. In the future, the integration of both parameters and train operation should be conducted from a long-term view to make a more comprehensive evaluation. Also, the optimal size of hybrid energy storage system can be further studied based on the model and results proposed in this study. By coordinating each component in the hybrid energy storage system, it is expected to exploit the advantages of different OESD and further enhance its energy saving capability in electrified railway systems.

REFERENCES

[1] A. González-Gil, R. Palacin, and P. Batty, "Sustainable urban rail systems: Strategies and technologies for optimal management of regenerative braking energy," *Energy conversion and management*, vol. 75, pp. 374–388, 2013.

[2] A. González-Gil, R. Palacin, P. Batty, and J. Powell, "A systems approach to reduce urban rail energy consumption," *Energy Conversion and Management*, vol. 80, pp. 509–524, 2014.

[3] T. Ratniyomchai, S. Hillmansen, and P. Tricoli, "Recent developments and applications of energy storage devices in electrified railways," *IET Electrical Systems in Transportation*, vol. 4, no. 1, pp. 9–20, 2013.

[4] R. Barrero, J. Van Mierlo, and X. Tackoen, "Energy savings in public transport," *IEEE vehicular technology magazine*, vol. 3, no. 3, pp. 26–36, 2008.

[5] R. Barrero, X. Tackoen, and J. Van Mierlo, "Stationary or onboard energy storage systems for energy consumption reduction in a metro network," *Proceedings of the Institution of Mechanical Engineers, Part F: Journal of Rail and Rapid Transit*, vol. 224, no. 3, pp. 207–225, 2010.

[6] M. Domnguez, A. Cucala, A. Fernndez, R. Pecharromn, and J. Blanquer, "Energy efficiency on train control: design of metro ato driving and impact of energy accumulation devices," in *9th World Congress on Railway Research WCRR 2011*, vol. 2011, 2011.

[7] M. Chymera, A. Renfrew, and M. Barnes, "Analyzing the potential of energy storage on electrified transit systems," in *8th World congress of railway research–WCRR*, vol. 2008, 2008.

[8] B. Destraz, P. Barrade, A. Rufer, and M. Klohr, "Study and simulation of the energy balance of an urban transportation network," in *2007 European conference on power electronics and applications*. IEEE, 2007, pp. 1–10.

[9] J.-P. Moskowitz and J.-L. Cohuau, "Steem: Alstom and ratp experience of supercapacitors in tramway operation," in *2010 IEEE Vehicle Power and Propulsion Conference*. IEEE, 2010, pp. 1–5.

[10] M. Ogasa, "Application of energy storage technologies for electric railway vehiclesexamples with hybrid electric railway vehicles," *IEEJ Transactions on Electrical and Electronic Engineering*, vol. 5, no. 3, pp. 304–311, 2010.

[11] A. Rufer, "Energy storage for railway systems, energy recovery and vehicle autonomy in europe," in *The 2010 International Power Electronics Conference-ECCE ASIA-*. IEEE, 2010, pp. 3124–3127.

[12] N. Ghaviha, J. Campillo, M. Bohlin, and E. Dahlquist, "Review of application of energy storage devices in railway transportation," *Energy Procedia*, vol. 105, pp. 4561 – 4568, 2017, 8th International Conference on Applied Energy, ICAE2016, 8-11 October 2016, Beijing, China.

[13] M. Spiryagin, P. Wolfs, F. Szanto, Y. Q. Sun, C. Cole, and D. Nielsen, "Application of flywheel energy storage for heavy haul locomotives," *Applied energy*, vol. 157, pp. 607–618, 2015.

[14] A. Rupp, H. Baier, P. Mertiny, and M. Secanell, "Analysis of a flywheel energy storage system for light rail transit," *Energy*, vol. 107, pp. 625–638, 2016.

[15] M. Miyatake and K. Matsuda, "Energy saving speed and charge/discharge control of a railway vehicle with on-board energy storage by means of an optimization model," *IEEJ Transactions on Electrical and Electronic Engineering*, vol. 4, no. 6, pp. 771–778, 2009.

[16] M. Miyatake and H. Ko, "Optimization of train speed profile for minimum energy consumption," *IEEJ Transactions on Electrical and Electronic Engineering*, vol. 5, no. 3, pp. 263–269, 2010.

[17] Y. Huang, L. Yang, T. Tang, Z. Gao, F. Cao, and K. Li, "Train speed profile optimization with on-board energy storage devices: A dynamic programming based approach," *Computers Industrial Engineering*, vol. 126, pp. 149 – 164, 2018.

[18] N. Ghaviha, M. Bohlin, and E. Dahlquist, "Speed profile optimization of an electric train with on-board energy storage and continuous tractive effort," in *2016 international symposium on power electronics, electrical drives, automation and motion (speedam)*. IEEE, 2016, pp. 639–644.

[19] C. Wu, W. Zhang, S. Lu, Z. Tan, F. Xue, and J. Yang, "Train speed trajectory optimization with on-board energy storage device," *IEEE Transactions on Intelligent Transportation Systems*, 2018.

[20] C. Wu, S. Lu, F. Xue, L. Jiang, and J. Yang, "Optimization of speed profile and energy interaction at stations for a train vehicle with on-board energy storage device," in *2018 IEEE Intelligent Vehicles Symposium (IV)*, June 2018, pp. 1–6.

[21] S. X. Chen, H. B. Gooi, and M. Q. Wang, "Sizing of energy storage for microgrids," *IEEE Transactions on Smart Grid*, vol. 3, no. 1, pp. 142–151, 2012.

[22] S. Bahramirad, W. Reder, and A. Khodaei, "Reliability-constrained optimal sizing of energy storage system in a microgrid," *IEEE Transactions on Smart Grid*, vol. 3, no. 4, pp. 2056–2062, 2012.

[23] T. K. Brekken, A. Yokochi, A. Von Jouanne, Z. Z. Yen, H. M. Hapke, and D. A. Halamay, "Optimal energy storage sizing and control for wind power applications," *IEEE Transactions on Sustainable Energy*, vol. 2, no. 1, pp. 69–77, 2011.

[24] E. Tara, S. Shahidinejad, S. Filizadeh, and E. Bibeau, "Battery storage sizing in a retrofitted plug-in hybrid electric vehicle," *IEEE Transactions on Vehicular Technology*, vol. 59, no. 6, pp. 2786–2794, 2010.

[25] M. Redelbach, E. D. Özdemir, and H. E. Friedrich, "Optimizing battery sizes of plug-in hybrid and extended range electric vehicles for different user types," *Energy Policy*, vol. 73, pp. 158–168, 2014.

[26] X. Hu, S. J. Moura, N. Murgovski, B. Egardt, and D. Cao, "Integrated Optimization of Battery Sizing, Charging, and Power Management in Plug-In Hybrid Electric Vehicles," *IEEE Transactions on Control Systems Technology*, vol. 24, no. 3, pp. 1036–1043, 2016.

[27] G. Graber, V. Calderaro, V. Galdi, A. Piccolo, R. Lamedica, and A. Ruvio, "Techno-economic sizing of auxiliary-battery-based substations in DC railway systems," *IEEE Transactions on Transportation Electrification*, vol. 4, no. 2, pp. 616–625, 2018.

[28] S. De La Torre, A. J. Sánchez-Racero, J. A. Aguado, M. Reyes, and O. Martínez, "Optimal Sizing of Energy Storage for Regenerative Braking in Electric Railway Systems," *IEEE Transactions on Power Systems*, vol. 30, no. 3, pp. 1492–1500, 2015.
[29] A. Ovalle, J. Pouget, S. Bacha, L. Gerbaud, E. Vinot, and B. Sonier, "Energy storage sizing methodology for mass-transit direct-current wayside support: Application to French railway company case study," *Applied Energy*, vol. 230, no. September, pp. 1673–1684, 2018.
[30] F. Ciccarelli, D. Iannuzzi, and P. Tricoli, "Control of metro-trains equipped with onboard supercapacitors for energy saving and reduction of power peak demand," *Transportation Research Part C: Emerging Technologies*, vol. 24, pp. 36–49, 2012.
[31] V. I. Herrera, H. Gaztañaga, A. Milo, A. Saez-De-Ibarra, I. Etxeberria-Otadui, and T. Nieva, "Optimal Energy Management and Sizing of a Battery-Supercapacitor-Based Light Rail Vehicle with a Multiobjective Approach," *IEEE Transactions on Industry Applications*, vol. 52, no. 4, pp. 3367–3377, 2016.
[32] M. Aneke and M. Wang, "Energy storage technologies and real life applications a state of the art review," *Applied Energy*, vol. 179, pp. 350 – 377, 2016.
[33] S. Koohi-Fayegh and M. Rosen, "A review of energy storage types, applications and recent developments," *Journal of Energy Storage*, vol. 27, p. 101047, 2020.
[34] R. Sioshansi and A. J. Conejo, *Mixed-Integer Linear Optimization*. Cham: Springer International Publishing, 2017, pp. 123–196.
[35] Y. Huang, X. Ma, S. Su, and T. Tang, "Optimization of train operation in multiple interstations with multi-population genetic algorithm," *Energies*, vol. 8, no. 12, pp. 14 311–14 329, 2015.
[36] K. Huang, J. Wu, X. Yang, Z. Gao, F. Liu, and Y. Zhu, "Discrete train speed profile optimization for urban rail transit: A data-driven model and integrated algorithms based on machine learning," *Journal of Advanced Transportation*, vol. 2019, 2019.

Chaoxian Wu was born in 1992 in Beihai, Guangxi, China. He received the BEng in Traffic Engineering from Tongji University, Shanghai, China. He was awarded his Intercollegiate MSc degree in Transport & Sustainable Development from Imperial College London, UK and University College London, UK. He is now pursuing the PhD of Electrical Engineering and Electronics from University of Liverpool, UK. His main research interests are railway engineering, train operation optimization, energy-saving strategies in transportation and smart transportation.

Shaofeng Lu is currently an associate professor with the Shien-Ming Wu School of Intelligent Engineering (WUSIE), South China University of Technology (SCUT), China. Before joining SCUT in 2019, he spent 6 years as a faculty member with Department of Electrical and Electronic Engineering, Xi'an Jiaotong-Liverpool University (XJTLU), China. He received the BEng and PhD degree from the University of Birmingham in 2007 and 2011 respectively. He also has a BEng degree from Huazhong University of Science and Technology, Wuhan, China. All are in Electrical and Electronic Engineering. His main research interests include power management strategies, railway traction system, electric vehicles, optimization techniques and energy-efficient transportation systems.

Fei Xue was born in 1977 in Tonghua of Jilin province in China. He received his Bachelor and Master degrees in power system and its automation from Wuhan University in China in 1999 and 2002, respectively. He received the Ph.D. of Electrical Engineering degree from the Department of Electrical Engineering of Politecnico di Torino, Torino, Italy, 2009. He was the Deputy Chief Engineer of Beijing XJ Electric Co.,Ltd and Lead Research Scientist in Siemens Eco-City Innovation Technologies (Tianjin) Co., Ltd. He is currently an associate professor with the Department of Electrical and Electronic Engineering, Xi'an Jiaotong-Liverpool University, No. 111 Ren'ai Road, Suzhou Industrial Park, Suzhou, P.R. China. His research interest focuses on power system security, virtual microgrids, transactive energy control and energy internet.

Lin Jiang received his B.S. and M.S. degrees from the Huazhong University of Science and Technology China; and his Ph.D. degree from the University of Liverpool UK, all in Electrical Engineering, in 1992, 1996 and 2001, respectively. He is presently working as a Reader of Electrical Engineering at the University of Liverpool. His current research interests include the optimization and control of smart grids, electrical machines, power electronics and renewable energy.

Minwu Chen received the B.Eng. and Ph.D. degrees in electrical engineering from Southwest Jiaotong University, Chengdu, China, in 2004 and 2009, respectively. From 2010 to 2012, he undertook postdoctoral researches in the China Railway First Survey and Design Institute Group, Xian, China. Since 2018, he has been a Full Professor at the School of Electrical Engineering, Southwest Jiaotong University, Chengdu, China. From 2014 to 2015, he was a Visiting Scholar at the University of Birmingham, Birmingham, UK. His research interests include new technology and power quality for railway traction systems.